Spine

SPINE Volume 37, Number 22, pp E1376–E1382

BASIC SCIENCE

Real-Time and Spatial Quantification Using Contrast-Enhanced Ultrasonography of Spinal Cord Perfusion During Experimental Spinal Cord Injury

Marc Soubeyrand, MD,*† Elisabeth Laemmel, PhD,* Arnaud Dubory, MS,*† Eric Vicaut, MD, PhD,* Charles Court, MD, PhD,† and Jacques Duranteau, MD, PhD*‡

Study Design. Experimental study in male Wistar rats.

Objective. To quantify temporal and spatial changes simultaneously in spinal cord blood flow and hemorrhage during the first hour after spinal cord injury (SCI), using contrast-enhanced ultrasonography (CEU).

Summary of Background Data. Post-traumatic ischemia and hemorrhage worsen the primary lesions induced by SCI. Previous studies did not simultaneously assess temporal and spatial changes in spinal cord blood flow.

Methods. SCI was induced at Th10 in 12 animals, which were compared with 11 sham-operated controls. Spinal cord blood flow was measured in 7 adjacent regions of interest and in the sum of these 7 regions. Blood flow was quantified using CEU with intravenous microbubble injection. Spinal cord hemorrhage was measured on conventional B-mode sonogram slices.

Results. CEU allowed us to measure the temporal and spatial changes in spinal cord blood flow in both groups. In the SCI group, spinal cord blood flow was significantly decreased in the global region of interest ($P = 0.0016$), at the impact site (epicenter), and in the 4 regions surrounding the epicenter, compared with the sham group. The blood flow decrease was maximum at the epicenter. No statistically significant differences between the sham groups were found for the most rostral and caudal regions of interest. Hemorrhage size increased significantly with time ($P < 0.0001$), from 30.3 mm^2 (±2) after 5 minutes to 39.6 mm^2 (±2.3) after 60 minutes.

Conclusion. CEU seems reliable for quantifying temporal and spatial changes in spinal cord blood flow. After SCI, bleeding occurs in the spinal cord parenchyma and increases significantly throughout the first hour.

Key words: spinal cord injury, regional blood flow, ischemia, ultrasonography, contrast agents. **Spine 2012;37:E1376–E1382**

Acute spinal cord injury (SCI) is a devastating event responsible for motor, sensory, and autonomic impairments. The annual incidence of SCI is estimated at 15 to 40 cases per million, and mean patient age is 33 years.[1,2]

The damage caused by SCI develops in 2 phases: the primary injury involves direct destruction of the cord parenchyma by the trauma, followed by the secondary injury in which various molecular and cellular events worsen the primary lesion.[3] Among the mechanisms responsible for the secondary injury, ischemia plays a major role in causing neuronal and glial necrosis.[4] At the epicenter of the injury, severe ischemia progresses inexorably to necrosis.[5] Surrounding this necrotic core, there is a zone of decreased blood flow that can progress either to severe ischemia and necrosis or to reperfusion and tissue survival.[6] Preservation of this zone may induce substantial clinical benefits. Thus, persistence of only 10% of myelinated motor axons was sufficient to enable walking in experimental animals.[7]

None of the techniques used to date to assess spinal cord blood flow in experimental settings provide simultaneous information on temporal and spatial changes in spinal cord blood flow. For example, laser Doppler, one of the most widely used techniques, allows real-time measurement of spinal cord blood flow[5,8,9] only to a depth of about 1 mm, that is, in only one-third of the diameter of the rat spinal cord.

Contrast-enhanced ultrasonography (CEU) is a recent method allowing *in vivo* quantification of tissue microperfusion on bidimensional slices. Microbubbles of encapsulated gas are injected to enhance blood-flow contrast within a tissue.[10] These microbubbles are safe in humans and are widely used to assess blood flow in tumors or organs.[11] However, to the best of our knowledge, CEU has not been used to investigate spinal cord blood flow.

Another factor that can dramatically aggravate SCI is bleeding within the spinal cord parenchyma. In rats, the presence

From the *Equipe Universitaire 3509, Paris VII – Paris XI – Paris XIII, Paris, France; †Service de Chirurgie Orthopédique; and ‡Département d'Anesthésie Réanimation, CHU Bicêtre, 78 Rue Général Leclerc, Le Kremlin-Bicêtre, France.

Acknowledgement date: May 16, 2012. Revision date: June 29, 2012. Acceptance date: July 4, 2012.

The manuscript submitted does not contain information about medical device(s)/drug(s).

No funds were received in support of this work.

One or more of the author(s) has/have received or will receive benefits for personal or professional use from a commercial party related directly or indirectly to the subject of this manuscript: *e.g.*, honoraria, gifts, consultancies, royalties, stocks, stock options, decision making position.

Address correspondence and reprint requests to Marc Soubeyrand, Equipe Universitaire 3509, Paris VII – Paris XI – Paris XIII, Paris, France; E-mail: soubeyrand.marc@wanadoo.fr

DOI: 10.1097/BRS.0b013e318269790f

of blood in the extravascular compartment triggers local vasospasm.[12,13] The size of the initial hemorrhagic focus correlates closely with subsequent changes in the necrotic area, which is seen as a spindle-shaped cavity.[14] In several clinical studies using magnetic resonance imaging (MRI), hemorrhage within the spinal cord was associated with poor neurological outcomes.[15] However, we are not aware of previous studies providing a detailed description of the spatial course of hemorrhage immediately after the trauma.

The goal of this experimental study was to quantify the temporal and spatial changes in blood flow and hemorrhage during the first hour following SCI. To this end, we used CEU in male Wistar rats.

MATERIALS AND METHODS

All the methods used in this experimental animal study were approved by the bioethics committee of the Lariboisière School of Medicine, Paris, France (CEEALV/2011–08-01). The animals were kept in individual cages in a room with a 12-hour light/dark cycle and free access to food and water.

Surgical Procedure

Male Wistar rats weighing 380 to 410 g were used (Figure 1). Thirty minutes after a subcutaneous buprenorphine injection (0.05 mg/kg), intraperitoneal sodium pentobarbital (60 mg/kg) was given for anesthetizing. To avoid hypothermia, the rat was placed on a heating blanket connected to a thermometric rectal probe in order to maintain temperature in the range of 37°C to 38°C. Tracheotomy was performed to permit ventilation with room air. A cannula inserted into the left carotid artery allowed monitoring of the mean arterial blood pressure (MABP) using Student Lab Pro software (Biopac Systems, Goleta, CA) and continuous hydration with 0.9% saline solution (10 mL/kg/hr).

The rat was placed in the prone position and a midline incision was performed. Localization of the 13th left rib allowed to identify precisely the thoracic (Th) vertebra Th13. The posterior arches were exposed from Th7 to Th13. Laminectomy with bilateral facetectomy was performed from Th8 to Th12, taking care to avoid damage to the neural roots and adjacent segmental arteries.

A stereotaxic frame was clamped to the spinous processes of Th6 and Th13 with the thorax elevated from the heating blanket to eliminate any influence of respiratory movements on spine position. Spine position was such that the spinal cord was strictly horizontal.

The ultrasound probe was positioned 5 mm from the spinal cord and in a parasagittal plane with 20° of left obliquity. Ultrasound gel between the cord and probe allowed the acquisition of a longitudinal cord slice while leaving free access to the posterior part of the cord. This ultrasound slice remained constant throughout the experiment, because the spine and ultrasound probe were locked into the stereotaxic frame.

At this point, a 30-minute hemodynamic stabilization phase was started. Five minutes after the end of this phase (defined as t0), a 10-g weight was dropped on the cord at Th10 from a height of 10 cm to induce severe SCI in 12 animals (SCI group). In 11 animals, no SCI was induced (sham group).

At the end of the experiment, the animal was killed with a lethal injection of pentobarbital IV.

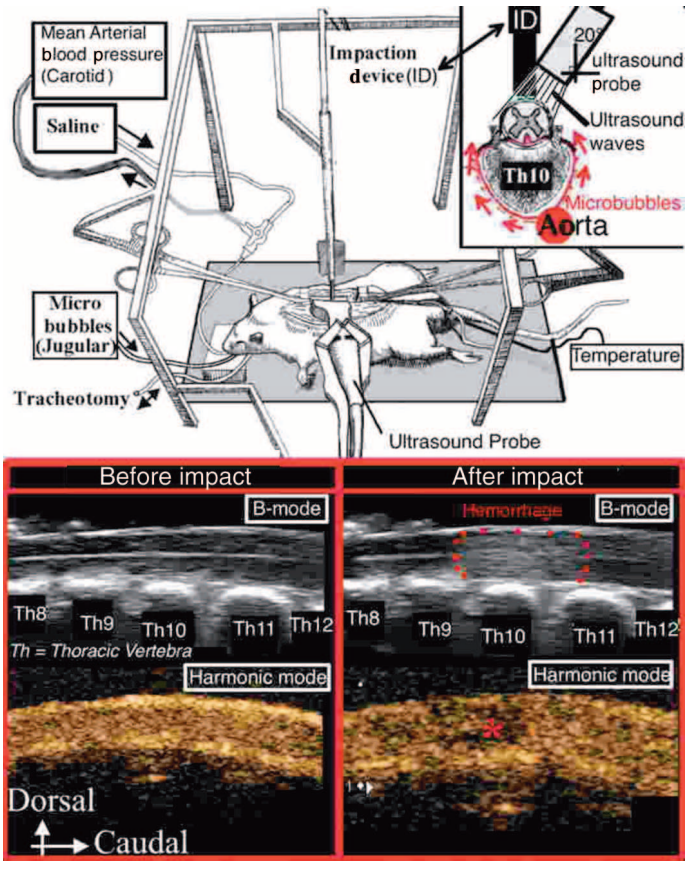

Figure 1. Schematic drawing of a rat in the stereotaxic frame. The ultrasound probe is oblique to allow positioning of the impaction device at the 10th thoracic vertebra (Th10). After the impact, hemorrhage is visible in B-mode. The harmonic mode shows the microbubbles (in orange). The asterisk indicates the necrotic core where ischemia is maximal.

Contrast-Enhanced Ultrasonography and Data Analysis

We used an Aplio ultrasound system (Toshiba, Tokyo, Japan). For each CEU, a bolus of 400 μL of Sonovue (Bracco Imaging, Milan, Italy) was injected intravenously. This contrast agent is composed of microbubbles filled with sulfur hexafluoride, ranging in size from 1 to 10 μm. The microbubbles reflect the ultrasound waves emitted by the probe, thereby increasing the echogenicity of the tissue. They can be destroyed by the high-frequency ultrasound waves used in conventional B-mode, but are spared by the lower frequency waves used in harmonic mode. Therefore, tissue blood flow can be quantified by computer analysis of the harmonic mode images. For each acquisition in our study, the ultrasound device was set on harmonic mode and 2 minutes of raw data were recorded automatically. Seven acquisitions were obtained in each animal. The first acquisition at the end of the 30-minute hemodynamic stabilization phase served to obtain baseline data. Then 5 acquisitions were obtained 5 (t5), 15 (t15), 30 (t30),

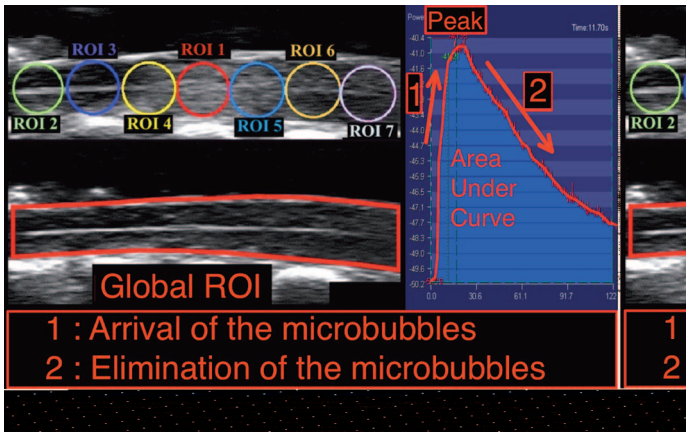

Figure 2. Spinal cord blood flow was assessed in 7 adjacent ROI, numbered 1 to 7, and in the sum of these 7 ROIs (global ROI). The software used for quantification delivers a typical curve with an ascending part corresponding to microbubble ingress and a descending part corresponding to microbubble egress.

45 (t45), and 60 (t60) minutes after the trauma or at the corresponding times in the sham group. Between acquisitions, the ultrasound system was switched to conventional B-mode for acquisition of morphological images and destruction of circulating microbubbles.

Each acquisition was analyzed using Ultra-Extend software (Toshiba, Tokyo, Japan). Spinal cord blood flow was quantified in 8 regions of interest (ROIs) positioned identically for each acquisition. The global ROI was the sum of the 7 other ROIs (ROIs 1–7), which were adjacent circles as shown in Figure 2. ROI 1 was at the level of the impact, that is, at the epicenter of traumatic damage. ROIs 2 through 4 were rostral to the epicenter, and ROIs 5 through 8 caudal to the epicenter. For each ROI and each acquisition from a baseline to t60, the software generated a perfusion-deperfusion curve and calculated the area under the curve (AUC) directly correlated to cord blood flow.

Temporo-Spatial Extent of the Hemorrhage

The size of the hemorrhagic area was measured using the Osirix software (Pixmeo, Geneva, Switzerland) on the conventional B-mode images, because the surface area in mm.[2] Hemorrhage size was determined at each time point from t0 to t60.

Statistical Analysis

Statistical analyses were performed using Statview 5.0 software (SAS Institute, Cary, NC). All results were reported as mean ± standard error of measurement.

To assess temporo-spatial changes in spinal cord blood flow, we computed the AUC in each ROI at each time point as a percentage of baseline (AUC%). Percentage variations in AUC were analyzed using repeated measures 3-way analysis of variance (ANOVA; time, ROI, and trauma/no trauma). When a significant interaction was found among the 3 factors, 2-way ANOVA (time, ROI, or trauma/no trauma) was used. To assess our hypothesis that hemorrhage size increased over time, we performed repeated measures 1-way ANOVA (time). When 2-way ANOVA was significant, *post hoc* analyses were performed using the Bonferroni comparison test. P values lower than 0.05 were considered statistically significant.

The same method was used to analyze MABP changes over time, with 2-way ANOVA.

RESULTS

In all animals, ultrasonography was constantly able to visualize the spinal cord from Th8 to Th12.

Temporal Evolution of MABP

Baseline MABP was similar in the 2 groups (107 ± 5 mmHg in the sham group *vs.* 109 ± 2 mmHg in the SCI group). Baseline AUCs were similar in the 2 groups for all ROIs.

Changes in Blood Flow

Blood flow in the global ROI decreased in both groups (Figure 3). However, the decrease was significantly higher in the SCI group than in the sham group (AUC, –65% ± 7% and –30% ± 10% at t60, $P = 0.0016$).

Blood flow changes in the individual ROIs 1 through 7 are illustrated in Figures 4 and 5. No significant differences were noted between the 2 groups for the ROIs located farthest from the epicenter (2 and 7). For the 5 remaining ROIs, blood flow was significantly decreased in the SCI group compared with the sham group (1, $P < 0.0001$; 3, $P = 0.0032$; 4,

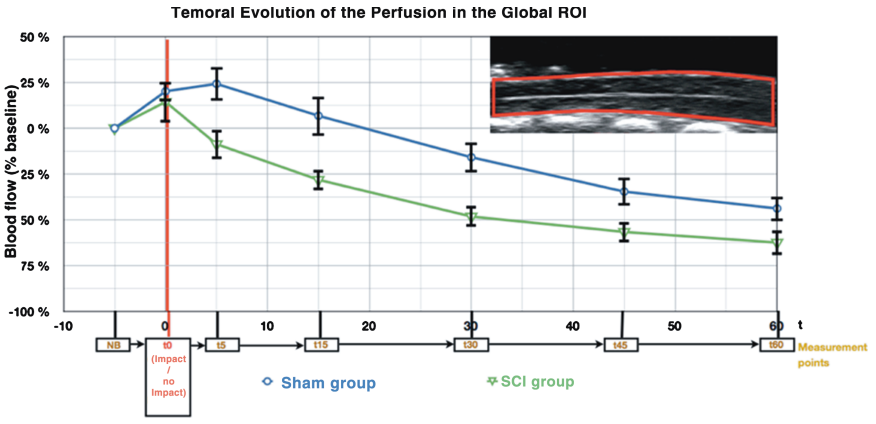

Figure 3. Blood flow in the global region of interest (ROI) in both groups.

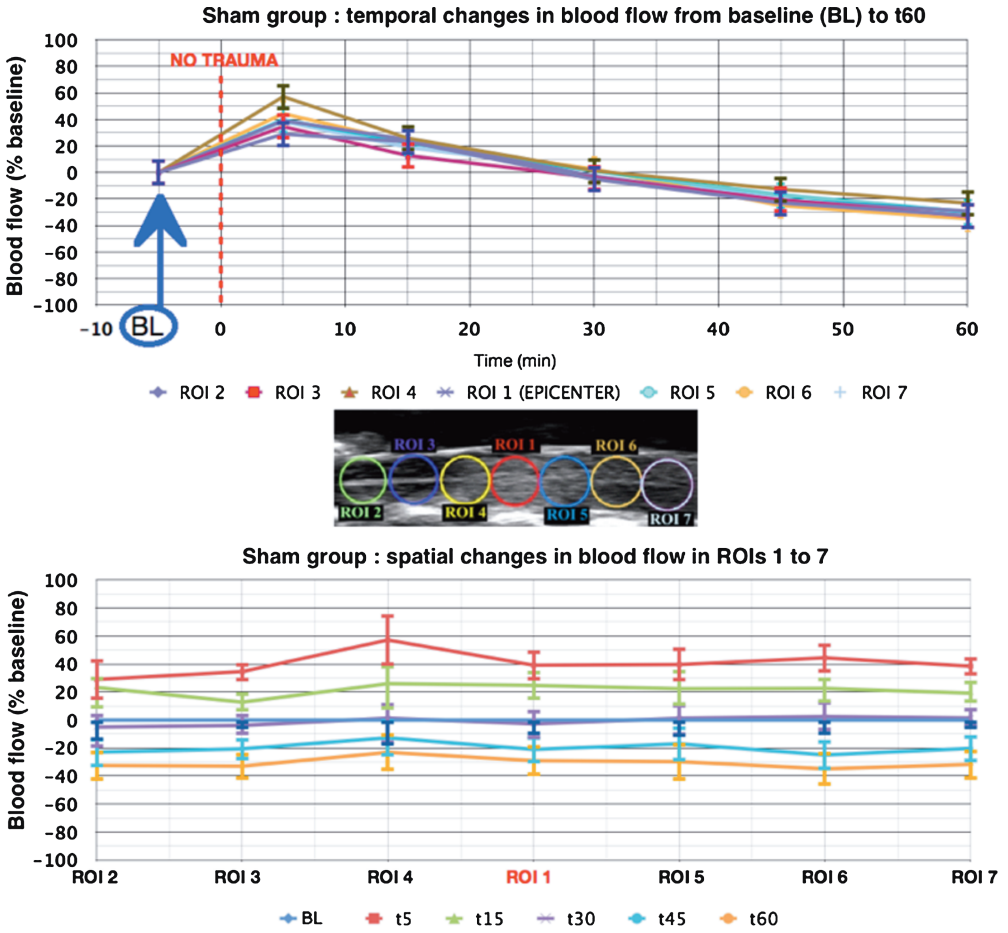

Figure 4. Changes in spinal cord blood flow in the regions of interest (ROIs) 1 through 7 in the sham-operated group.

$P = 0.0001$; 5, $P = 0.0364$; and 6, $P = 0.0252$). The difference was maximum for ROI 1 (epicenter), where blood flow at t60 was diminished by 93% ± 12% in the SCI group *versus* 29% ± 11% in the sham group (a 64% difference). At the epicenter, the blood flow decrease was maximum during the first 30 minutes after the trauma.

Temporo-Spatial Extent of the Hemorrhage

Hemorrhage size increased significantly ($P < 0.0001$) over time, from 30.3 ± 2 mm^2 at t5 to 36.7 ± 2.2 mm^2 at t20 and 39.6 ± 2.3 mm^2 at t60. The increase was maximum during the first 30 minutes after the trauma (Figure 6).

DISCUSSION

We found that spinal cord blood flow decreased significantly between Th8 and Th12 during the hour following SCI at Th10. The spatial blood flow pattern was valley-shaped, with the epicenter having the lowest value and the most distant areas (in the rostral and caudal directions) having the highest values. At the epicenter, the blood flow decrease was maximum during the first 30 minutes after SCI. To the best of our knowledge, this is the first detailed description of temporo-spatial blood flow changes after SCI. Moreover, conventional B-mode ultrasonography consistently showed bleeding that started in the epicenter and extended subsequently, particularly during the first 30 minutes after SCI.

At the epicenter, 60 minutes after SCI, blood flow was decreased by 64% compared with the sham group. Similarly, a study of spinal cord blood flow assessed using the hydrogen clearance method after severe clip compression trauma in rats showed a 70% decrease at the epicenter.[16] Blood flow decreases at the epicenter were 60% after severe weight-dropping SCI in a canine model[17] and 66% after severe SCI in a monkey model.[18]

Our results demonstrate that after SCI 3 territories can be defined according to their blood flows: (1) the epicenter, where blood flow was lowest (corresponding to our ROI 1); (2) the territories adjacent to the epicenter caudally and cranially, where blood flow was significantly decreased (our ROIs 3 and 4 rostrally and 5 and 6 caudally); and (3) the intact cord, where blood flow was unchanged after SCI (our ROIs 2 and 7, showing no significant difference with the sham group). Our model allows blood flow quantification within these 3 territories after severe SCI. At the epicenter, direct mechanical destruction of the neurovascular tissues occurs.[4] Conversely, in the second territory, the penumbra concept described for ischemic stroke[19] may be relevant: functionally impaired tissue can survive and recover if sufficient blood flow is restored promptly. Although this second territory is small, salvaging it may generate considerable clinical benefits. Thus, in a cat model, sparing only 10% of motor axons was enough to allow locomotion.[7] Ischemia is defined as

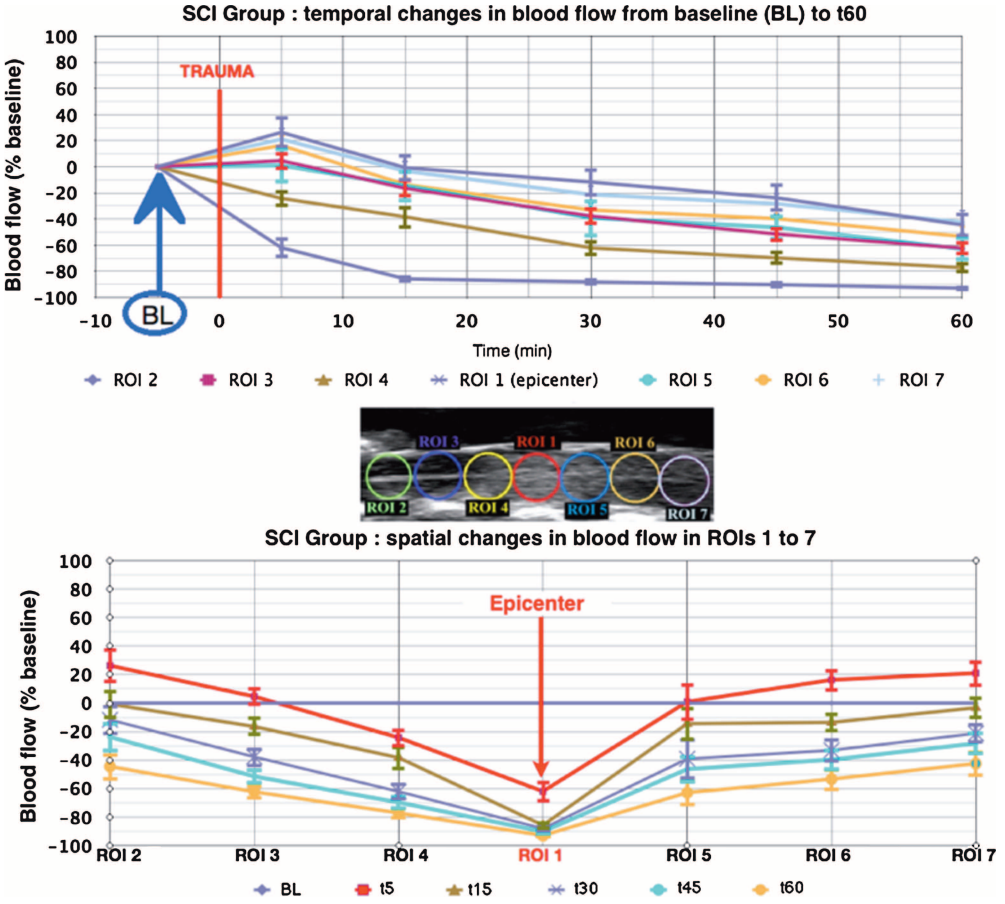

Figure 5. Changes in spinal cord blood flow in the regions of interest (ROIs) 1 through 7 in the group with induced spinal cord injury (SCI). Ischemia was most marked at the epicenter (ROI 1) and blood flow increased gradually in the rostral and caudal directions.

blood flow impairment causing cell dysfunction. The result may be either cell function recovery or cell necrosis, depending on the severity and duration of ischemia. The threshold for irreversible ischemic damage varies across components of the central nervous system.[20] However, the site with the maximum blood flow impairment undergoes necrotic cell death within a few minutes.[21] In the past, cell death after ischemia was ascribed only to necrosis. However, research conducted in the past decade has shown that neurons in the ischemic penumbra can undergo apoptosis, mediated in part by proteins belonging to the caspase family.[22] The latter can serve as therapeutic targets to reduce the extent of the lesions, and therefore it emphasizes the importance of studying ischemia in SCI.

To our knowledge, CEU has not been used previously to measure spinal cord blood flow. Previous studies used the radioactive tracer microsphere technique[23,24] laser Doppler flowmetry,[5,25] the hydrogen clearance technique,[26] and C14-iodoantipyrine autoradiography.[27] All these techniques have specific limitations. For example, the hydrogen clearance technique requires electrode insertion into the spinal cord, which may in theory modify spinal cord blood flow. With laser Doppler, blood flow is measured within a half-sphere about 1 mm in diameter, which precludes a full evaluation of the 3-mm wide rat spinal cord. With both techniques, the number of measurement points is limited by the number of available probes/electrodes. Conversely, CEU allows real-time, repeated, *in vivo* measurements of blood flow all along a spinal cord segment. The cord and surrounding dura can be left intact. Moreover, the same device used for CEU can provide morphologic images when used in conventional B-mode, whereas other techniques for assessing blood flow provide only functional information. Finally, with CEU, the raw data can be processed as many times as needed using specific software to modify the size, shape, and location of the ROIs. However, CEU has its limitations, for example, intravenous

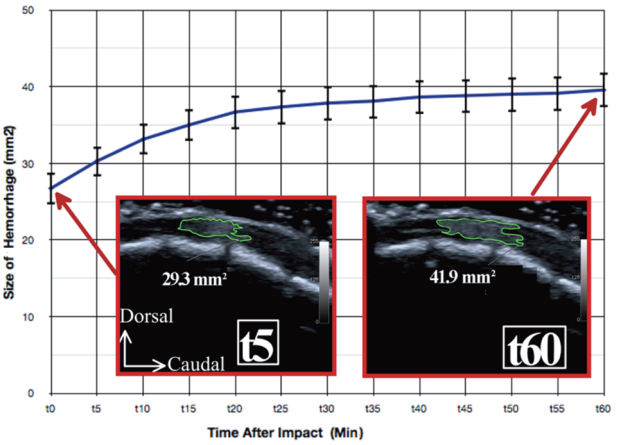

Figure 6. Changes in hemorrhage size over time.

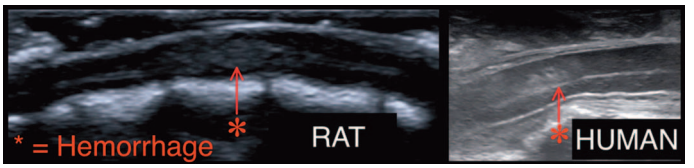

Figure 7. Appearance of the hemorrhage obtained using B-mode ultrasonography in a rat with spinal cord injury and in a human patient with spinal cord contusion responsible for paraplegia after a burst fracture of the 11th thoracic vertebra.

microbubble injections are required at each time point. Cord blood flow is thus studied at multiple time points, as opposed to monitoring continuously because the ultrasound device and microbubbles are expensive.

With the conventional B-mode, we were able to measure the size repeatedly of the cord hemorrhage induced by SCI. Thus, we were able to correlate real-time morphological information with functional data. Until now, data on post-SCI hemorrhage came only from postmortem histological studies, and therefore no information was available on the real-time course of bleeding *in vivo*. In clinical practice, magnetic resonance imaging of bleeding within the injured spinal cord correlates with poor neurological outcomes.[15] Interestingly, the morphological ultrasound findings in our model closely resembled those seen in patients with SCI (Figure 7). Intraoperative ultrasound examination of the spinal cord (*i.e.*, after the laminectomy) is safe as the probe can be positioned remote from the dura with an interface of physiological saline. In the future, it should be interesting to assess the capacity of this technique to refine the neurological prognosis: the extent of both parenchymal hemorrhage (*i.e.*, on conventional B-mode) and penumbra zone (*i.e.*, on CEU) through the motor and sensitive tracts of white matter may be correlated with the neurological outcomes.

The main limitation of our study is the change in spinal cord blood flow induced by the sham operation. Spinal cord blood flow increased from t0 to t15, then decreased by about 30% from t15 to t60, whereas MABP remained unchanged. Conceivably, repeated microbubble destruction within spinal cord capillaries may gradually injure the vessel walls. Because microbubble destruction is obtained using high-frequency ultrasound, we plan to test this hypothesis in a further study by modifying the frequencies used and destroying the microbubble elsewhere than in the spinal cord. The decrease in SCBF found in the present study is consistent with the findings of Anderson *et al*,[28] who used an isotope-labeled microspheres technique and found that an isolated laminectomy can generate a significant decrease (22%–45%) of SCBF during the minutes following the procedure. These authors ignored the pathophysiology of this "laminectomy-induced" decline in SCBF but have suggested a mechanism of temperature-induced vasoconstriction. Despite this limitation, the time-course of spinal cord blood flow was highly reproducible across animals. Moreover, our model was able to show a significant difference between sham and SCI groups.

CONCLUSION

We established that CEU can provide quantitative real-time and spatial data on spinal cord blood flow. SCI was followed by blood flow impairment that was maximum at the epicenter and decreased in the rostral and caudal directions. Moreover, cord hemorrhage size as assessed using conventional B-mode ultrasonography increased throughout the 60 minutes following SCI, with the maximum increase being noted in the first 30 minutes.

➢ Key Points

- ❑ Contrast-enhanced ultrasonography seems reliable for quantifying spinal cord blood flow under experimental conditions.
- ❑ B-mode ultrasonography visualizes the parenchymal hemorrhage induced by experimental spinal cord injury.
- ❑ Spinal cord blood flow decreases within the first 60 minutes after spinal cord injury, and the decrease is maximum at the epicenter.
- ❑ The size of the parenchymal hemorrhage increases significantly during the first 60 minutes after spinal cord injury.

Acknowledgment

Charles Court and Jacques Duranteau have contributed equally to this work.

References

1. Sekhon LH, Fehlings MG. Epidemiology, demographics, and pathophysiology of acute spinal cord injury. *Spine (Phila Pa 1976)* 2001;26:S2–12.
2. Wyndaele M, Wyndaele JJ. Incidence, prevalence and epidemiology of spinal cord injury: what learns a worldwide literature survey? *Spinal Cord* 2006;44:523–9.
3. Cadotte DW, Fehlings MG. Spinal cord injury: a systematic review of current treatment options. *Clin Orthop Relat Res* 469: 732–41.
4. Mautes AE, Weinzierl MR, Donovan F, et al. Vascular events after spinal cord injury: contribution to secondary pathogenesis. *Phys Ther* 2000;80:673–87.
5. Hamamoto Y, Ogata T, Morino T, et al. Real-time direct measurement of spinal cord blood flow at the site of compression: relationship between blood flow recovery and motor deficiency in spinal cord injury. *Spine* 2007;32:1955–62.
6. McDonald JW, Sadowsky C. Spinal-cord injury. *Lancet* 2002;359:417–25.
7. Blight AR. Cellular morphology of chronic spinal cord injury in the cat: analysis of myelinated axons by line-sampling. *Neuroscience* 1983;10:521–43.
8. Horn EM, Theodore N, Assina R, et al. The effects of intrathecal hypotension on tissue perfusion and pathophysiological outcome after acute spinal cord injury. *Neurosurg Focus* 2008;25:E12.
9. Carlson GD, Gorden CD, Nakazawa S, et al. Sustained spinal cord compression: part II: effect of methylprednisolone on regional blood flow and recovery of somatosensory evoked potentials. *J Bone Joint Surg Am* 2003;85-A:95–101.
10. Postema M, Schmitz G. Bubble dynamics involved in ultrasonic imaging. *Expert Rev Mol Diagn* 2006;6:493–502.
11. Quaia E. Microbubble ultrasound contrast agents: an update. *Eur Radiol* 2007;17:1995–2008.

12. Wallace MC, Tator CH, Frazee P. Relationship between posttraumatic ischemia and hemorrhage in the injured rat spinal cord as shown by colloidal carbon angiography. *Neurosurgery* 1986;18:433–9.
13. Bullock R, Fujisawa H. The role of glutamate antagonists for the treatment of CNS injury. *J Neurotrauma* 1992;9:S443–62.
14. Noble LJ, Wrathall JR. Correlative analyses of lesion development and functional status after graded spinal cord contusive injuries in the rat. *Exp Neurol* 1989;103:34–40.
15. Bozzo A, Marcoux J, Radhakrishna M, et al. The role of magnetic resonance imaging in the management of acute spinal cord injury. *J Neurotrauma*;28:1401–11.
16. Guha A, Tator CH, Rochon J. Spinal cord blood flow and systemic blood pressure after experimental spinal cord injury in rats. *Stroke* 1989;20:372–7.
17. Griffiths IR, Trench JG, Crawford RA. Spinal cord blood flow and conduction during experimental cord compression in normotensive and hypotensive dogs. *J Neurosurg* 1979;50:353–60.
18. Ducker TB, Assenmacher DR. Microvascular response to experimental spinal cord trauma. *Surg Forum* 1969;20:428–30.
19. Heiss WD. The concept of the penumbra: can it be translated to stroke management? *Int J Stroke* 2010;5:290–5.
20. Mattson MP, Duan W, Pedersen WA, et al. Neurodegenerative disorders and ischemic brain diseases. *Apoptosis* 2001;6:69–81.
21. Ginsberg MD. The new language of cerebral ischemia. *AJNR Am J Neuroradiol* 1997;18:1435–45.
22. Broughton BR, Reutens DC, Sobey CG. Apoptotic mechanisms after cerebral ischemia. *Stroke* 2009;40:e331–9.
23. Bassingthwaighte JB, Malone MA, Moffett TC, et al. Validity of microsphere depositions for regional myocardial flows. *Am J Physiol* 1987;253:H184–93.
24. Drescher WR, Weigert KP, Bunger MH, et al. Spinal blood flow in 24-hour megadose glucocorticoid treatment in awake pigs. *J Neurosurg* 2003;99:286–90.
25. Westergren H, Farooque M, Olsson Y, et al. Spinal cord blood flow changes following systemic hypothermia and spinal cord compression injury: an experimental study in the rat using Laser-Doppler flowmetry. *Spinal Cord* 2001;39:74–84.
26. Ueda Y, Kawahara N, Tomita K, et al. Influence on spinal cord blood flow and function by interruption of bilateral segmental arteries at up to three levels: experimental study in dogs. *Spine (Phila Pa 1976)* 2005;30:2239–43.
27. Golanov EV, Reis DJ. Contribution of oxygen-sensitive neurons of the rostral ventrolateral medulla to hypoxic cerebral vasodilatation in the rat. *J Physiol* 1996;495:201–16.
28. Anderson DK, Nicolosi GR, Means ED, et al. Effects of laminectomy on spinal cord blood flow. *J Neurosurg* 1978;48:232–8.